

Self-construction of Magnetic Hollow $\text{La}_{0.7}\text{Sr}_{0.3}\text{MnO}_3$ Microspheres with Complex Units

Xuefeng Chu, Keke Huang, Mei Han, and Shouhua Feng*

State Key Laboratory of Inorganic Synthesis and Preparative Chemistry, College of Chemistry, Jilin University, Changchun 130012, People's Republic of China

Supporting Information

ABSTRACT: Perovskite structure $\text{La}_{0.7}\text{Sr}_{0.3}\text{MnO}_3$ magnetic hollow microspheres with complex units were prepared via the hydrothermal route without hard and soft templates. The formation of hollow microspheres follows the self-construction mechanism involving oriented attachment, dissolution, and recrystallization processes. It exhibits a ferromagnetic behavior at room temperature.

Hollow structures have attracted considerable attention in the synthesis of functional materials for their promising applications in vastly different fields in the past decade.^{1–4} Although the template method is common and effective,⁵ the high cost of templates and multistep synthetic procedures have proven very difficult to overcome. The template-free method was considered to be one of the simplest alternatives to get hollow structures and to avoid these disadvantages.^{6,7} However, this strategy is only useful for some certain special compounds. It is noted that, among known preparative hollow materials, most of the pioneers reported that results are limited in simple compositions and simple geometrical shapes. Although some multicomponent hollow materials were synthesized in the past few years,^{8–10} preparing hollow complex oxides is still a challenge at present because of the complexity of the reaction system. To explore new capabilities of hollow structure materials, researchers are seeking novel and simple approaches to hollow structures with multicompositions and complex geometrical shapes.

Herein, we use $\text{La}_{0.7}\text{Sr}_{0.3}\text{MnO}_3$ (typical perovskite manganese oxide with potential application for its high Curie temperature, colossal magnetoresistance effect, oxidation catalytic performance, and half-metallic nature^{11–13}) to demonstrate that hollow spheres with complex units can be prepared via a simple hydrothermal route from a concentrated KOH solution without any hard or soft templates.

X-ray diffraction (XRD) measurement of the product, as shown in Figure 1, indicated a monoclinic phase feature with space group $P21/a$, and all peaks were in good agreement with the document value (JCPDS card no. 49-0595). Inductively coupled plasma elemental analysis confirmed the energy-dispersive spectrometry (EDS) result (Figure S1 in the Supporting Information, SI) and indicated that the composition of the product was $\text{La}_{0.7}\text{Sr}_{0.3}\text{MnO}_3$.

Figure 2a shows a scanning electron microscopy (SEM) image of $\text{La}_{0.7}\text{Sr}_{0.3}\text{MnO}_3$ hollow microspheres with uniform diameter of ca. 20 μm . Typical hollow microsphere architecture

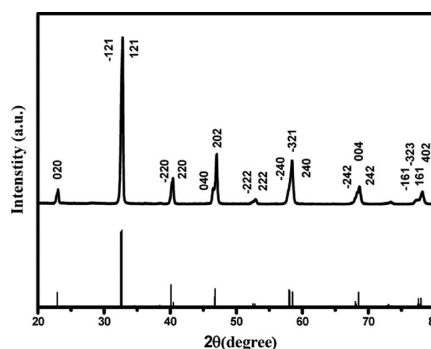


Figure 1. Powder XRD pattern of the product and reference of JCPDS card no. 49-0595.

is observed at different magnifications and visual angles in Figure 2b,c. Detailed views on the shell structure indicate that the $\text{La}_{0.7}\text{Sr}_{0.3}\text{MnO}_3$ hollow microspheres are comprised of numerous complex building units as external cubes and internal nanoaggregations, as shown in Figure 2d,e. The specific surface area measured with the Brunauer–Emmett–Teller technique is ca. 1.44 m^2/g , and the pore size is 2.5 nm obtained by a pore-size distribution curve (Figure S2 in the SI). A cross-sectional high-resolution transmission electron microscopy (HRTEM) image of the hollow $\text{La}_{0.7}\text{Sr}_{0.3}\text{MnO}_3$ shell is shown in Figure 2f. HRTEM of the hollow sphere shell shows consecutive lattice fringes arranged in order without any crystalline border. The space of the observed lattice fringes was deduced to be 0.39 nm, which was associated with the (020) lattice plane of the monoclinic phase.

The formation of $\text{La}_{0.7}\text{Sr}_{0.3}\text{MnO}_3$ hollow spheres was affected by some factors such as the alkalinity concentration and reaction time. By keeping the reaction time for 72 h, it was indicated that the KOH concentration plays a key role. The lower alkalinities of 20 and 25 g (7.5 and 9.2 M) lead to the cubic phase and low-dimensional structure, and the higher alkalinities of 30 and 40 g (11.0 and 14.7 M) lead to the monoclinic phase and complex hollow structure (Figures S3 and S4 in the SI). The combined structure of nanobuilding and cubic particles, as shown in Figure S4a in the SI, indicated that cubic particles were probably grown from nanorods and nanoparticles through aggregation and recrystallization processes.

Received: December 4, 2012

Published: March 27, 2013

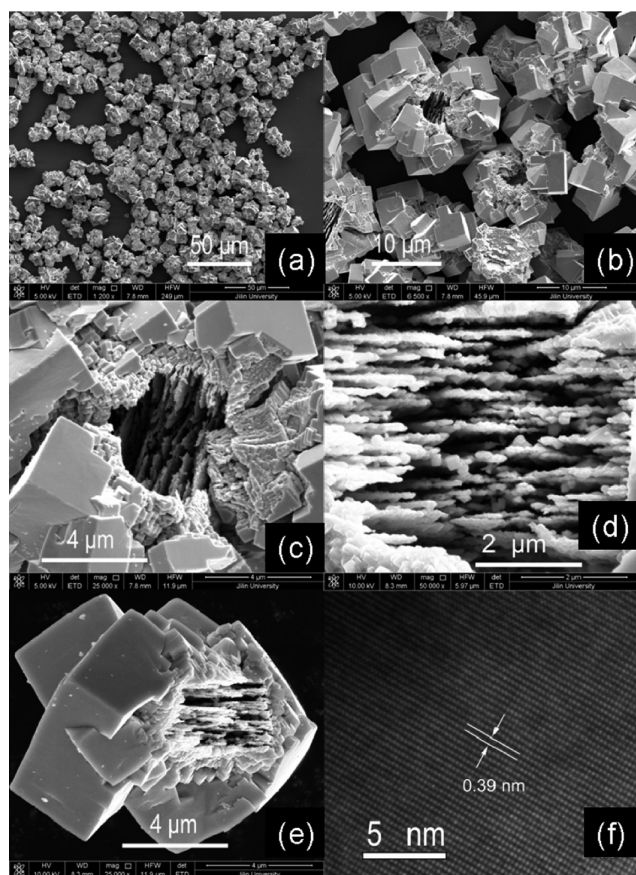


Figure 2. SEM images of $\text{La}_{0.7}\text{Sr}_{0.3}\text{MnO}_3$ micrometer hollow architectures from different magnifications and visual angles: (a) low-magnification SEM image; (b and c) high-magnification SEM images; (d) internal morphology; (e) complex microbuilding unit; (f) cross-sectional HRTEM image of the sphere shell.

To gain further insight into the formation process, the intermediate products with different growth times with certain 30 g (11.0 M) KOH were also investigated. When the hydrothermal reaction was run within 1 or 2 h, none of the products presented. Microplates consisting of cubes were the main products after 3 h, as shown in Figure 3a. By extension of the reaction time to 7 h, the plates developed and internal nanostructures appeared (Figure 3b). At the reaction stage of 7 h, as shown in Figure 3c, the cubic particles connected together to form the framework. Upon further extension of the time to 18 h, part of sphere appeared toward the half-sphere after 36 h with great cave and apparent internal platelike nanoaggregations, as shown in Figure 3d,e. Upon further extension to 72 h, the products showed apparently hollow spheres with complex external and internal units, as shown in Figures 1b,c and 3f. XRD patterns, as shown in Figure S5 in the SI, illustrated that all products are well crystallized, as seen by the fact that the intensity of the (040) peaks gradually increased with the reaction time, which is more or less dependent on the formation degree of hollow sphere structures.

The formation mechanism of $\text{La}_{0.7}\text{Sr}_{0.3}\text{MnO}_3$ complex hollow microspheres was thus proposed to follow the “bottom-up”-oriented attachment and recrystallization processes. This mechanism has been widely applied to other systems with hollow structure.^{14–16} The proposed formation process is illustrated in Figure 4. In the early stage, cubic micro and nano building units generated and attached to each other, forming

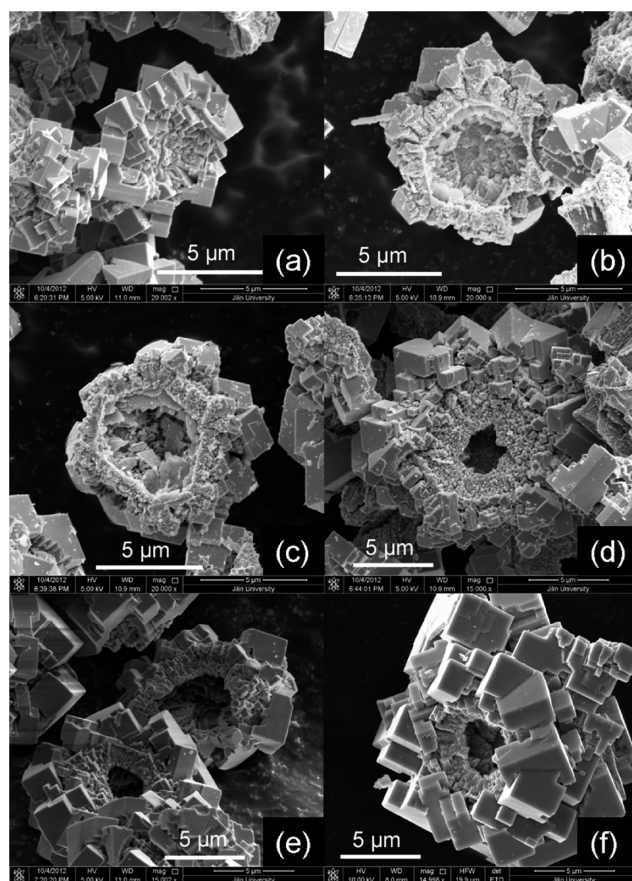


Figure 3. Typical SEM images of products synthesized at the same alkalinity as 30 g of KOH (11.0 M) for different reaction times such as (a) 3, (b and c) 7, (d) 18, (e) 36, and (f) 72 h.

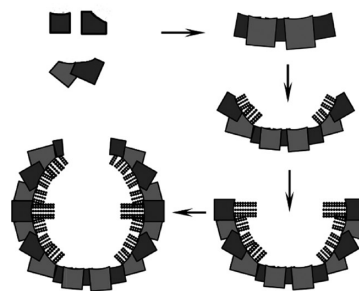


Figure 4. Schematic illustration of a cross-sectional view of the proposed growth process of the hollow spheres with complex units.

two-dimensional plates. Notably, the building units are very sensitive to the alkalinity condition. At this stage, the building units might be small, and further attachment on the edge extended the plate. Outside crystals have enough space to grow, but inside crystals have no space to grow and dissolve because of their small size in the process of crystallization. Further attachment on the plate edge enlarged the particle size and finally led to the hollow sphere structure. The attachment depended on the active faces available on the primary nano/microcrystallites, which were determined by alkalinity conditions. There was also attachment of nanoparticles inside the spheres, which connected and grew to smooth faces in the recrystallization process without protection of the shell (Figure 3a). Further growth and recrystallization enlarge the building units, as reported in a previous work.¹⁶ When the time was

prolonged, the shell became apparent, whereas the nano-aggregation including robs and plates remained to weaken the recrystallization effect inside the hollow spheres due to the confinement of the shell. The crystal growth processes are certainly very complicated, and it may involve at least three processes such as dissolution, recrystallization, and “bottom-up”-oriented attachment. Therefore, further study on the formation process is still needed.

Figure 5a presents zero-field-cooled (ZFC) and field-cooled (FC) magnetization plots measured from 4 to 400 K in an

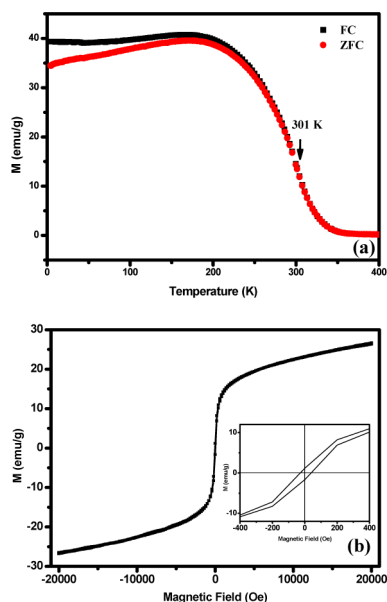


Figure 5. (a) ZFC and FC magnetization plots in the temperature range from 4 to 400 K under a 0.1 T field. (b) Field dependence of the magnetization curves for the hollow sphere samples (-20 and $+20$ kOe) at 300 K.

applied field of 0.1 T. The obvious transition from ferromagnetism to paramagnetism with a Curie temperature of ca. 301 K is observed in Figure 5a. Our value for T_c is lower compared to that previously reported by Zi et al. ($T_c = 367$ K), where $\text{La}_{0.7}\text{Sr}_{0.3}\text{MnO}_3$ nanoparticles were prepared by the chemical coprecipitation route.¹⁷ It seems that T_c for $\text{La}_{1-x}\text{Sr}_x\text{MnO}_3$ compounds is affected by the size and shape of the sample.¹⁸ Figure 5b presents $M-H$ curves of the sample at 300 K. The $M-H$ curves clearly are irreversible, which is consistent with the room-temperature ferromagnetism due to the double exchange of Mn^{3+} and Mn^{4+} (the mixed valence of Mn^{3+} and Mn^{4+} was observed as shown in Figure S6 in the SI).¹⁹ The magnetic property of the hollow spheres may make the sample sensitive to an external magnetic field.

In summary, we have prepared a complex componential- and geometrical-shaped hollow sphere of $\text{La}_{0.7}\text{Sr}_{0.3}\text{MnO}_3$ without any templates by the ready hydrothermal method. In the synthesis, the concentrated KOH is a key factor. The formation processes are complicated and may combine processes such as dissolution, recrystallization, and attachment. The hollow sphere exhibits a ferromagnetism behavior at room temperature.

■ ASSOCIATED CONTENT

📄 Supporting Information

Experimental details and nitrogen adsorption, EDS, XRD, SEM, and X-ray photoelectron spectroscopy data. This material is available free of charge via the Internet at <http://pubs.acs.org>.

■ AUTHOR INFORMATION

Corresponding Author

*E-mail: shfeng@mail.jlu.edu.cn.

Notes

The authors declare no competing financial interest.

■ ACKNOWLEDGMENTS

This work was supported by the National Natural Science Foundation of China (Grants 90922034, 21131002, and 21201075) and Specialized Research Fund for the Doctoral Program of Higher Education (SRFDP Grant 20110061130005).

■ REFERENCES

- (1) Lou, X. W.; Archer, L. A.; Yang, Z. C. *Adv. Mater.* **2008**, *20*, 3987.
- (2) Lai, X. Y.; Halpert, J. E.; Wang, D. *Energy Environ. Sci.* **2012**, *5*, 5604.
- (3) Zhao, Y.; Jiang, L. *Adv. Mater.* **2009**, *21*, 3621.
- (4) Hu, J.; Chen, M.; Fang, X.; Wu, L. *Chem. Soc. Rev.* **2011**, *40*, 5472.
- (5) Jiao, S.; Xu, L.; Jiang, K.; Xu, D. *Adv. Mater.* **2006**, *18*, 1174.
- (6) Zhao, H.; Chen, J. F.; Zhao, Y.; Jiang, L.; Sun, J. W.; Yun, J. *Adv. Mater.* **2008**, *20*, 3682.
- (7) Jia, C. J.; Sun, L. D.; Yan, Z. H.; You, L. P.; Luo, F.; Han, X. D.; Pang, Y. C.; Zhang, Z.; Yan, C. H. *Angew. Chem., Int. Ed.* **2005**, *44*, 4328.
- (8) Yang, X. F.; Williams, I. D.; Chen, J.; Wang, J.; Xu, H. F.; Konishi, H.; Pan, Y. X.; Liang, C. L.; Wu, M. M. *J. Mater. Chem.* **2008**, *18*, 3543.
- (9) Dong, Z.; Ye, T.; Zhao, Y.; Yu, J.; Wang, F.; Zhang, L.; Wang, X.; Guo, S. *J. Mater. Chem.* **2011**, *21*, 5978.
- (10) Ye, T.; Dong, Z.; Zhao, Y.; Yu, J.; Wang, F.; Guo, S.; Zou, Y. *CrystEngComm* **2011**, *13*, 3842.
- (11) Tokura, Y. *Rep. Prog. Phys.* **2006**, *69*, 797.
- (12) Park, J.-H.; Vesocovo, E.; Kim, H.-J.; Kwon, C.; Ramesh, R.; Venkatesan, T. *Nature* **1998**, *392*, 794.
- (13) Liang, S. H.; Teng, F.; Bulgan, G.; Zhu, Y. F. *J. Phys. Chem. C* **2007**, *111*, 16742.
- (14) Zeng, H. C. *J. Mater. Chem.* **2011**, *21*, 7511.
- (15) Liu, B.; Zeng, H. C. *Chem. Mater.* **2007**, *19*, 5824.
- (16) Chen, X. Y.; Qiao, M. H.; Xie, S. H.; Fan, K. N.; Zhou, W. Z.; He, H. Y. *J. Am. Chem. Soc.* **2007**, *129*, 13305.
- (17) Zi, Z. F.; Sun, Y. P.; Zhu, X. B.; Hao, C. Y.; Luo, X.; Yang, Z. R.; Dai, J. M.; Song, W. H. *J. Alloys Compd.* **2009**, *477*, 414.
- (18) Spooren, J.; Walton, R. I.; Millange, F. *J. Mater. Chem.* **2005**, *15*, 1542.
- (19) Zener, C. *Phys. Rev.* **1951**, *82*, 403.